Hindawi
Journal of Chemistry
Volume 2018, Article ID 5395106, 12 pages
https://doi.org/10.1155/2018/5395106

Research Article

Synthesis and Voltammetric Determination of Pb(II) Using a ZIF-8-Based Electrode

Dinh Quang Khieu,[1] **Mai Thi Thanh**,[1,2] **Tran Vinh Thien**,[3] **Nguyen Hai Phong**,[1] **Duc Hoang Van**,[4] **Pham Dinh Du**,[5] **and Nguyen Phi Hung**[6]

[1]*University of Sciences, Hue University, Hue 530000, Vietnam*
[2]*Faculty of Physics-Chemistry-Biology, Quang Nam University, Tam Ky 560000, Vietnam*
[3]*Faculty of Natural Science, Phu Yen University, Phu Yen 620000, Vietnam*
[4]*University of Education, Hue University, Hue 530000, Vietnam*
[5]*Faculty of Natural Sciences, Thu Dau Mot University, Thu Dau Mot 820000, Vietnam*
[6]*Department of Chemistry, Quy Nhon University, Quy Nhon 590000, Vietnam*

Correspondence should be addressed to Dinh Quang Khieu; dqkhieu@hueuni.edu.vn

Received 24 October 2017; Accepted 12 April 2018; Published 10 May 2018

Academic Editor: Fateme Razeai

Zeolite imidazole framework-8 (ZIF-8) was prepared by the hydrothermal process. The obtained ZIF-8 was a characteristic of X-ray-diffraction (XRD), transmission electron microscope (TEM), thermal gravity-differential thermal analysis (TG-DTA), and dynamic light scattering (DLS). The obtained ZIF-8 possessed large specific area and was highly dispersed. Its morphology consisted of nanospherical particles with 30–50 nm in diameter. Chemical stability of ZIF-8 in different conditions was studied. The ZIF-8 was used as an electrode modifier for the determination of trace levels of lead. The parameters including solvents and solution pH were investigated. The repeatability, reproducibility, accuracy, linear range, limit of detection, and limit of quantitation were also addressed. The results showed that ZIF-8 is a potential electrode modifier for differential pulse anodic stripping method to determine Pb(II) in aqueous solution.

1. Introduction

Metal-organic frameworks (MOFs) are gaining significant attention for their potential applications in gas separation and storage, sensors, and catalysis [1–3] during the last years. Zeolite imidazole frameworks ZIF-8, being a kind of MOFs, consist of Zn atoms linked through nitrogen atoms by 2 methyl-imidazole (denoted as Im) links to create neutral frameworks and to provide tunable nanosized pores formed by four-, six-, eight-, and twelve-membered ring ZnN_4 [4]. ZIF-8 has appeared as a novel kind of highly porous materials combining desirable properties from both zeolites and conventional MOFs including high surface areas, crystallinity, thermal, and chemical stability [4–7]. ZIF-8 is a promising class of nanoporous materials for gas separating membrane [5, 8], gas adsorption, storage of hydrogen [9, 10], and catalysts [11–13].

Heavy metals (Hg(II), Pb(II), Cd(II), Ni(II), and so on) are considered to be one of the main sources of pollution in the environment. Lead is one of the most dangerous environmental pollutants as it has toxic chemical influence even at very small concentration [14, 15]. So it is urgently needed to find a very sensitive method for the determination of lead trace in the environment. Several analytical techniques, such as spectroscopic methods, especially graphite furnace atomic adsorption spectroscopy (GF-AAS) [16], inductively coupled plasma mass spectroscopy (ICP-MS) [17], and X-ray fluorescence [18], are employed currently for trace analysis of lead. These methods have excellent sensitivities and good selectivity; but several disadvantages such as time-consuming and high cost of instrument limit their applications.

Electrochemical methods including anodic stripping voltammetric techniques (ASV) have been recognized as robust tools for trace analysis because of different advantages such as faster analysis, higher selectivity and sensitivity, low cost, easy operation, and possibility to perform analysis in situ [19, 20]. Differential pulse anodic stripping voltammetry

(DP-ASV), as one kind of the ASV method, has been applied for the determination of trace heavy metal ions because of its remarkably high sensitivity. Glassy carbon electrodes chemically modified with porous materials such as modified mesoporous materials [21], clay-mesoporous silica composite [22], multiwall carbon nanotubes [14], reduced graphene oxide/chitosan [23], pretreated graphite pencil [24], graphene films [25], and polyaniline and polypyrrole film [26] have received considerable attention for ASV because they exhibit significant improvements in terms of fast response, high selectivity, low detection limit, and renewability.

Due to high surface areas, highly order structure, and high reactive site density, the usage of MOFs-based composite for the electrochemical field is becoming increasing. Mao et al. [27] reported the usage of copper (II)-2,2′-bipyridine-benzene-1,3,5-tricarboxylate (Cu(II) based MOF-199) as selective electrocatalysts for the reduction of O_2 and CO_2. MOF modified by Au-SH-SiO2 nanoparticles was utilized to determinate hydrazine and L-cysteine by electrochemistry analysis [28]. The amino-functionalized MOF-199 material could provide an excellent modifier for developing a sensitive electrode for the determination of lead trace [29]. Ag-loaded ZIF-8 nanocrystals were used as an electrode modifier to detect hydrazine. Ag/ZIF-8/CPE (carbon paste electrode) performed a good catalytic performance toward hydrazine oxidation [30]. Xiao et al. [20] reported the nitrogen-doped microporous carbon prepared from pyrolysis of ZIF-8 as an excellent electrode modifier to determine Pb(II) and Cd(II) in aqueous solution.

In the previous paper [31], we demonstrated the using of ZIF-8-modified electrode to determine Pb(II) in aqueous solution. In the present work, we continue to refine the study on the use of ZIF-8 as an electrode modifier for the determination of Pb(II) by the voltammetric technique. The stability of ZIF-8 over time in several solvents and in different pH solutions was studied. ZIF-8 has been used to modify the glassy carbon electrode (GCE) for Pb(II) determination using DP-ASV methods. Several parameters related to the electrode performance were studied and optimized for using in the analysis. To our knowledge, this is the first report on using modified electrode-based ZIF-8 material for the determination of lead by the DP-ASV.

2. Experimental

2.1. Materials. Zinc nitrate hexahydrate ($Zn(NO_3)_2{\cdot}6H_2O$, Daejung, Korea), methanol (CH_3OH, Merck, Germany), and 2-methylimidazole ($C_4H_6N_2$, Aldrich, USA) were utilized in the synthesis of ZIF-8. For electrochemistry performance, bismuth(III) nitrate pentahydrate ($Bi(NO_3)_3{\cdot}5H_2O$, Sigma-Aldrich, USA) was used to prepare the bismuth film. Nafion solution was prepared from stock solution (5%, $d = 0.874\ g{\cdot}mL^{-1}$, Aldrich, USA) and ethanol (96%, Merck, Germany) with a volume ratio $V_{nafion}/V_{ethanol}$: 1/4. Britton–Robinson buffer solution (B-R BS) of pH = 4.7 was prepared from 0.04 M H_3BO_3, 0.04 M H_3PO_4, and 0.04 M CH_3COOH (Merck, Germany). pH of the B-R BS was adjusted by the addition of 1.0 M sodium hydroxide solutions into the B-R BS and then checked by the pH meter. The working solution of Pb(II) was prepared daily from stock solution (1000 ppm, Merck, Germany).

2.2. Synthesis of ZIF-8. ZIF-8 was synthesized according to [32–34]. Briefly, zinc nitrate (2.8 mmol) was dissolved in methanol (1.4 mL). 2-Methylimidazole (64.4 mmol) was dissolved in methanol (1.4 mL), and this solution was added to the zinc solution under sonication condition for 30 minutes and then vigorously stirred for 24 h at room temperature. Finally, this solution was centrifuged at 300 rpm and washed thoroughly with methanol. This washing procedure was repeated 5 times. The resulting crystals were dried overnight at 120°C.

2.3. Voltammetric Procedure

2.3.1. Preparation of Working Electrode-Modified Electrodes. The preparation procedure was carried out as in [28]. In brief, glassy carbon electrode (GCE) was first polished with 0.05 μm Al_2O_3 slurry on a polishing cloth and then rinsed ultrasonically with 2 M HNO_3, absolute ethanol, and double-distilled water. Subsequently, the GCE was electrochemically cleaned by a cyclic potential scan between −1.1 V and +0.3 V in 0.5 M acetate buffer solution pH 4.5 with the scan rate of $0.10\ V{\cdot}s^{-1}$. After that, the electrode was rinsed with double-distilled water. The nafion/ZIF-8 composite was prepared by dispersing 2.5 mg ZIF-8 into 1.0 mL nafion (0.1 wt.%) and sonicated. The GCE was coated with 5 μL of the nafion/ZIF-8 composite and dried under the room temperature (~25°C) (denoted as Naf/ZIF-8/GCE). For the same procedure, the GCE modified by nafion was denoted as Naf/GCE. Bismuth film (BiF) was formed simultaneously with Pb(II) preconcentration. The bismuth deposition was conducted at −1.2 V potential under stirring for 120 s. The GCE, Naf/GCE, and Naf/ZIF-8/GCE modified by BiF were denoted as BiF/GCE, Naf/BiF/GCE, and Naf/BiF/ZIF-8/GCE, respectively.

2.3.2. Voltammetric Procedure. Solution under study (final volume of 10 mL) containing 0.04 M B-R BS (pH 4.7) and 200 ppb Pb(II) was transferred into the electrochemical cell with the 3 electrodes. Then, voltammetric measurement was conducted as follows:

(i) For surveying voltammetric characteristics of Pb(II) on the modified GCE: Pb(II) was accumulated on the surface of the modified electrode at a potential of −1.2 V (E_{acc}) for an accumulated time of 120 s (t_{acc}). During this step, the electrode was rotated at a constant rate of 1000 rpm. After that, the electrode rotation was off, and then, cyclic voltammograms (CVs) were recorded from −1.1 V to +0.3 V (forward potential scan) and then from +0.3 V to −1.1 V (reverse potential scan) at a scan rate of $0.1\ V{\cdot}s^{-1}$.

(ii) For differential pulse anodic stripping voltammetric (DP-ASV) determination of Pb(II) on modified GCE: during the DP-ASV procedure, Pb(II) was accumulated on the surface of the rotating modified

electrode as done for the above procedure. After that, the electrode rotation was off for 10 s, and then, DP-ASV voltammograms were recorded from −1.1 V to +0.3 V at a scan rate of 0.02 V·s^{-1}. DP-ASV voltammograms of blank solution (without Pb(II) and prepared from double-distilled water) were similarly recorded before each measurement.

2.4. Apparatus. XRD was performed by powder X-ray diffraction (XRD), recorded on 8D Advance Bucker, Germany, with CuK_α radiation. Thermal behavior of ZIF-8 was analyzed by thermal analysis (TG-DTA) using Labsys TG Setaram (France) under air atmosphere. Morphology was observed by scanning electron microscopy using Jeol Jem-2100F TEM (Japan). Particle sizes were analyzed by DLS with Nanobrook 90plus PALS. A CPA-HH5 Computerized Polarography Analyzer (Vietnam) was used for voltammetry experiments. All measurements were done in the cell with three electrodes: a GCE with a diameter of 2.8 ± 0.1 mm used for formatting the modified electrode as a working electrode, a Ag/AgCl/3 M KCl as a reference electrode, and a platinum wire as an auxiliary electrode. All measurements were carried out at room temperature.

3. Results and Discussion

3.1. Synthesis of ZIF-8

3.1.1. Characterization of ZIF-8. The XRD pattern of ZIF-8 is shown in Figure 1. The XRD pattern of ZIF-8 was agreed well with patterns from [34–36], and no obvious peaks of impurities can be detected in the XRD patterns. There are well-defined diffractions (011), (022), (112), (022), (013), (224), (114), (233), (134), and (334) at two theta of 7.2, 10.1, 12.7, 14.9, 16.1, 22.1, 24.9, 25.5, and 26.5 degree, respectively, in the XRD pattern of ZIF-8 indicating that the crystallinity of ZIF-8 in this work was relatively high.

TEM observation of ZIF-8 is presented in Figure 2(a). The morphology of ZIF-8 consisted of nanospherical particles around 30–40 nm in diameter. The crystallite size was evaluated by Sherrer's equation from the peak (011). The crystallite size of ZIF-8 was 49.4 nm. The particle size was also analyzed by DLS as shown in Figure 2(b). The distribution curve exhibited the symmetric bell-shape indicating that the particle size had normal distributions. The agglomerate mean size of ZIF-8 estimated by DLS was 70.7 nm. The size calculated by DLS is the agglomerate size (grain size) which is formed from single particles. The single particles observed by the TEM consisted of crystallites. The crystallite size was calculated by XRD. The fact the mean size calculated by XRD is similar to that calculated by TEM indicates that the single phase of ZIF-8 with high crystallinity was obtained. Since the agglomerate sizes are only approximately 1.5–2 times the size of particle or crystallite size the agglomerates observed by the TEM are loosen and highly dispersible.

The nitrogen sorption study for the ZIF-8 reveals a reversible type I isotherm, a characteristic of microporous materials (not shown here). The sample of ZIF-8 possessed

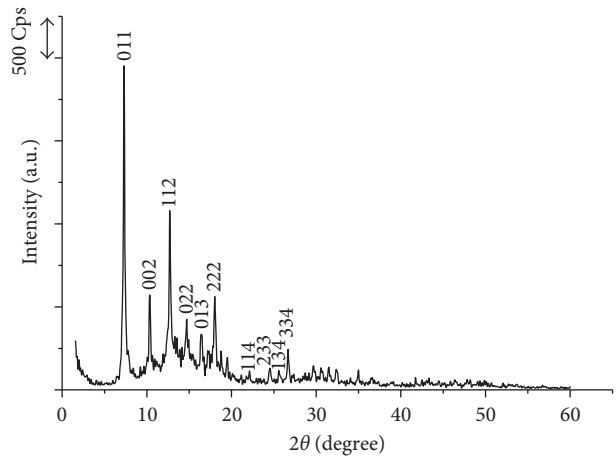

Figure 1: XRD pattern of ZIF-8.

the high specific surface area of 1484 m^2·g^{-1} and the total volume of 1.16 cm^3·g^{-1}, which was similar or higher with that in the previous literatures [35–37].

3.1.2. Stability of ZIF-8. The stability of ZIF-8 in different conditions is important for its application in catalyst as well as an electrode modifier. In present paper, the effects of time, solvents, and pH on the ZIF-8 structure were investigated.

Figure 3(a) shows XRD patterns of ZIF-8 exposed to ambient atmosphere for 1–12 months. The characteristic diffractions of ZIF-8 were unchangeable indicating that ZIF-8 was stable in ambient condition for a year. The chemical stability of ZIF-8 was investigated in refluxing C_2H_5OH, H_2O, and C_6H_6 at boiling temperature as shown in Figure 3(b). XRD patterns showed that ZIF-8 maintained full crystallinity for 8 hours at boiling conditions.

XRD patterns of ZIF-8 submerged in water at room temperature for 1–14 days are shown in Figure 4(a). XRD patterns collected at designated intervals showed that ZIF-8 was stable in water for at least 14 days. ZIF-8 was soaked in water with pH ranging from 2 to 12 for 24 hours. XRD analyses (Figure 4(b)) showed that characteristic peaks of ZIF-8 submerged in pH 2 solution were not observed implying that ZIF-8 was unstable in this condition. However, it was stable in the pH ranging from 2.7 to 12.

3.2. Electrochemical Performance of ZIF-8-Based Modified Electrodes

3.2.1. Selection of Experimental Conditions. In order to verify the electrochemical activity of ZIF-8 in the modified GCE for detection of Pb(II), the electrochemical experiments in GCE modified with and without ZIF-8 were performed by DP-ASVs. As can be seen in Figure 5(a), the stripping voltammetry peak varied from −0.624 to −0.586 V indicating that E_p of Pb(II) depended on the kind of working electrodes. The nafion was added because nafion membrane can be used as a coating to limit the interference of surface-active compounds as well as a stabilizer to improve the mechanical stability of the bismuth film electrode [38]. The

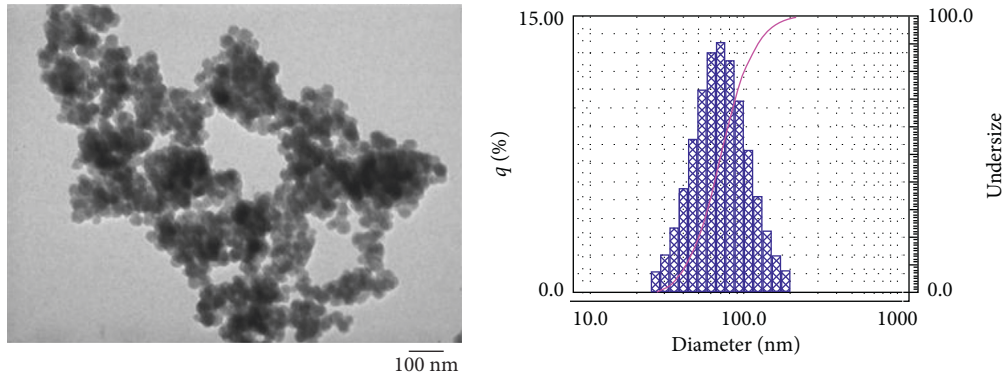

(a) (b)

Figure 2: TEM observation (a) and size distribution curve (b) of ZIF-8.

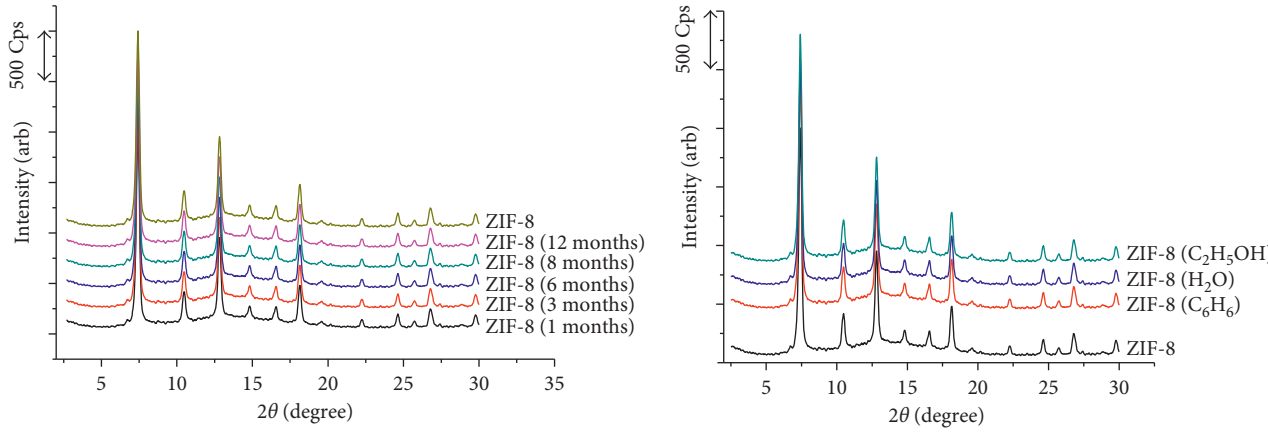

(a) (b)

Figure 3: XRD patterns of ZIF-8 in ambient atmosphere (a); ZIF-8 in refluxing some boiling solvents for 10 hours (b).

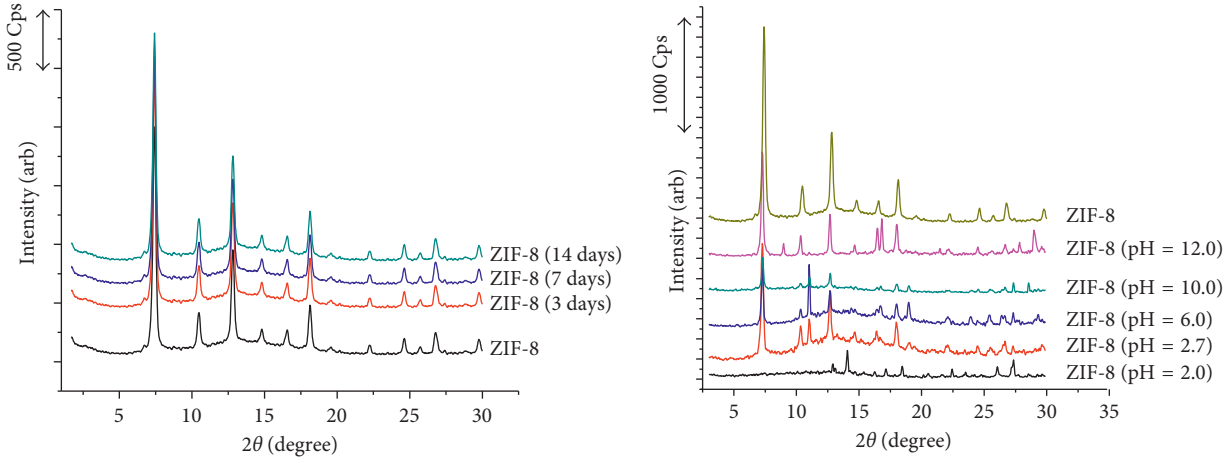

(a) (b)

Figure 4: XRD patterns of ZIF-8 submerged in water at room temperature (a) and water with different pHs (b).

current response on the Naf/GCE (curve c) and the bare GCE (curve e) exhibited the broad peaks, especially on Naf/GCE was almost not detectable. By the addition of ZIF-8, the current response at Naf/ZIF-8/GGE provided a well-defined peak as that at BiF/GCE which is widely used in DP-ASV for the determination of Pb(II). It is worth noting that

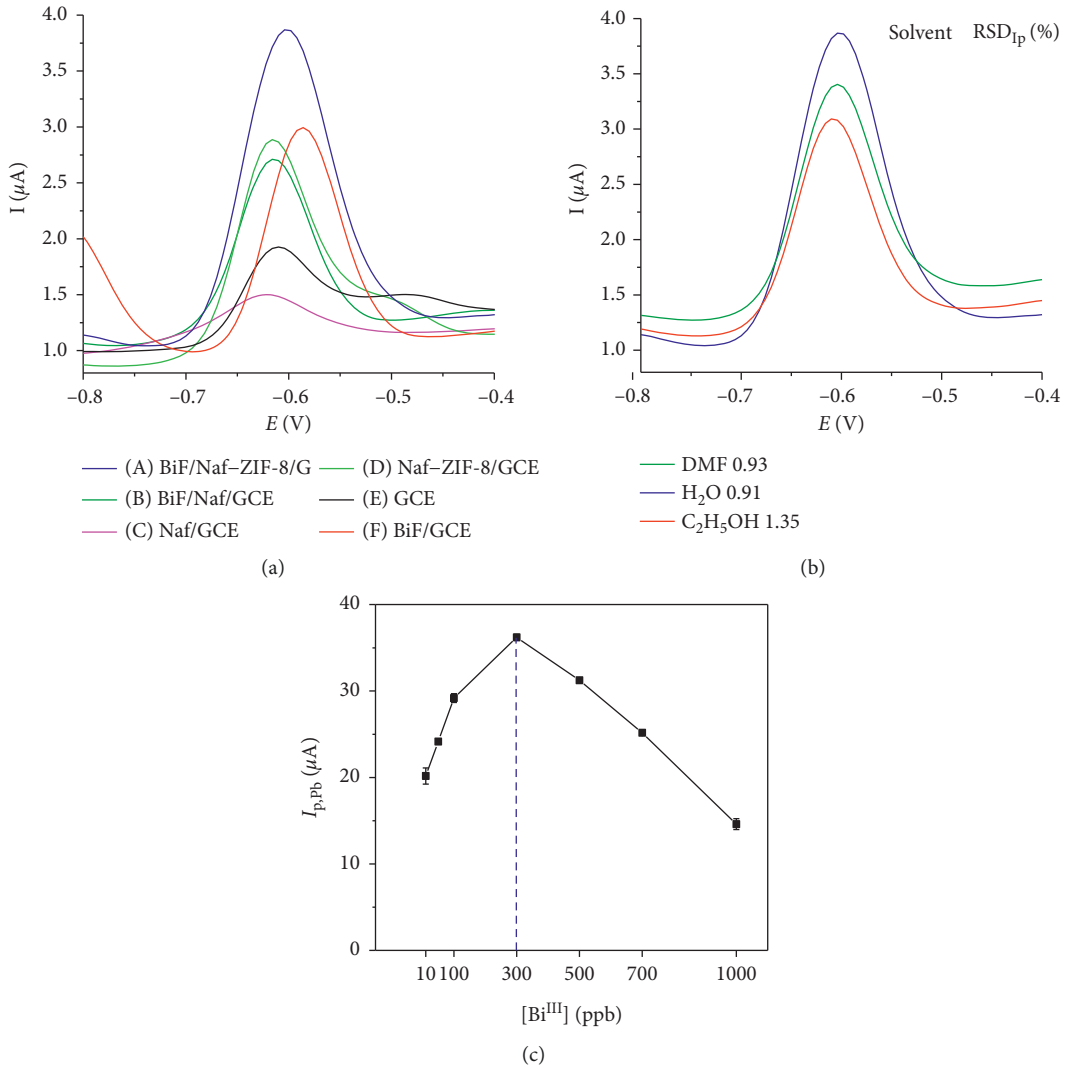

Figure 5: (a) DP-ASVs of Pb(II) (50 ppb) in acetate buffer solution (pH 4.7) at BiF/Naf/ZIF-8/GCE (A), BiF/Naf/GCE (B), Naf/GCE (C), Naf/ZIF-8/GCE (D), bare GCE (E), and BiF/GCE (F). (b) Anodic stripping current (I_p) of Pb(II) for DMF, H_2O, and C_2H_5OH solvent; (c) I_p of Pb(II) versus Bi(III) concentration for preparing the BiF film on the electrode Pb(II): 50 ppb; acetate buffer (pH = 4.7); $V_{ZIF\text{-}8} = 5\,\mu L$ (2.5 mg of ZIF-8/1 mL DMF).

adding ZIF-8 and incorporating the bismuth film exhibited the well-defined stripping signal with highest intensity. The intensity of I_p (peak current) at BiF/Naf/ZIF-8/GCE was 1.82-fold when compared with that at BiF/GCE as well as Naf/ZIF-8/GCE.

The favorable signal-promoting effect of the ZIF-8 indicated that it could accelerate the rate of electron transfer of Pb(II) and had good electrocatalytic activity for the *redox* reaction of Pb(II). The porous structure of ZIF-8 with the binding properties of the nitrogen group provides a high number of reactive sites that are ready for accessing the target analyte (Pb(II)). This synergistic combination of these effects leads to a greater amount of lead accumulation on the surface of BiF/Naf/ZIF-8/GCE, greatly improving its stripping peak current. The solvent for dispersing ZIF-8 often effects significantly on the current peak (I_p). Three solvents (e.g., dimethylformamide (DMF), water, and ethanol) were used to disperse ZIF-8. The signals I_p were presented at Figure 5(b). The results showed that water was favorable for dispersing ZIF-8 because it provided highest I_p with lowest (relative standard deviation) $RSD_{ip} = 0.9$. Therefore, water was selected as a dispersion solvent for further studies. The concentration of Bi(III) in analytical solution may influence the properties of the in situ bismuth film on GCE and effect on the accumulation efficiency and DP-ASV method. As seen from Figure 5(c), the stripping peak currents increased with the Bi(III) concentration from 0 to 300 ppb and decreased in the range 300 to 600 ppb with the peak at 300 ppb. The decreasing of the stripping peak currents after peak being reached was due to hindering mass transfer caused by too thick bismuth film. Therefore, the optimized concentration of bismuth was chosen as 300 ppb of Bi(III) for further study.

The effect of pH on the response of Pb(II) has been conducted in the pH ranging from 2.6 to 5.6 as shown in Figure 6(a). It was noted that the anodic peak current increases with increasing pH from 2.6 to 3.3. A further increase

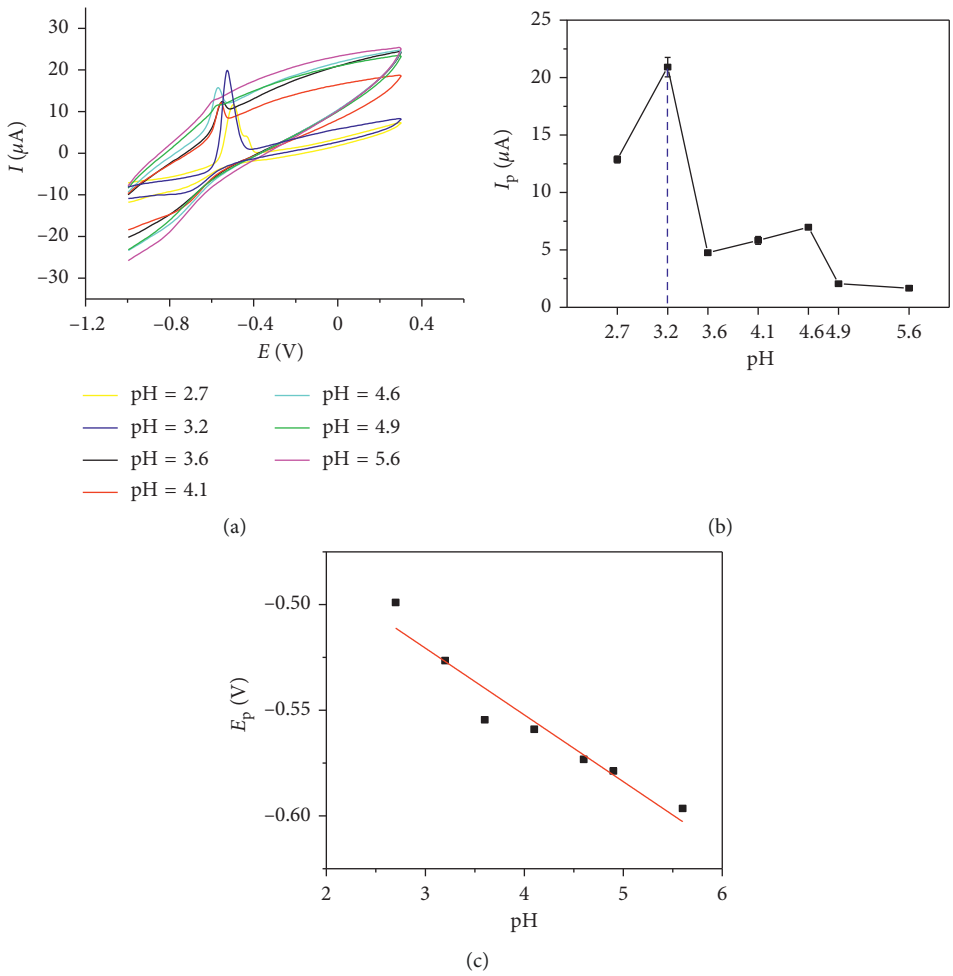

FIGURE 6: (a) Anodic stripping current (I_p) of Pb(II) at different pHs and condition: [Pb(II)]: 500 ppb; [Bi(III)] = 300 ppb. (I_p was the mean value for successive measurements for four times); (b) effect of pH on I_p of anodic peak; (c) linear regression of E_p versus pH.

in the pH leads to a decline of the current. These observations might be explained as follows: at low pH, the signal intensity of lead was low, which was due to the protonated amino groups repulsing with the cations via electrostatic repulsion. With the increase of pH, the protonated amino groups decrease, and electrostatic attraction results in a higher stripping current of lead. The best signal intensity with low RSD_{Ep} (4.4%) is reached at pH = 3.3. The pH = 3.3 was chosen for the optimal pH. The relationship between pH and anodic peak potential, E_p, is shown in Figure 6(b). As can be seen, anodic peak potential shifts negatively with increasing pH from 2.7 to 5.6 suggesting that protons involved directly to lead oxidation or the oxidation was hindered at low concentrations of protons The linear regression equation can be expressed as follows:

$$E_p\,(\text{mV}) = (-0.031 \pm 0.010)\text{pH} - (-0.428 \pm 0.041) \quad (R = -0.9651,\ p \le 0.001), \tag{1}$$

where E_p is the anodic peak potential and R is the relation coefficient.

The linear relation between E_p and pH is significant ($R = -0.9651$, $p \le 0.001$) (Figure 6(c)). The slope of regression is close to the theoretical value of $1/2 \times 0.0599$ (25°C). It is possible that the electrochemical process has the involvement of a proton and two electrons.

3.2.2. Effects of Scan Rate. Important information about the electrochemical mechanism can usually be obtained from the relationship between peak current and scan rate. Therefore, the effect of scan rate on E_p and I_p was investigated by CV as shown in Figure 7. If the electrooxidation reaction is irreversible, then E_p is dependent on v. As can be seen from Figure 7(a), peak potential shifts to higher potential as scan rate increases, and then it is concluded that electron transfer in Pb(II) electrooxidation is irreversible. Peak current increases with an increase in the scan rate from 20–500 $\text{mV}\cdot\text{s}^{-1}$ (Figure 7(b)) suggesting that the electron transfer reaction involved with a surface-confined process [39].

In order to determine if the electrooxidation reaction is adsorption or diffusion controlled, the plots of peak current (I_p) against square root of the scan rate ($v^{1/2}$) and $\ln I_p$ against $\ln v$ are performed in Figure 8. If a plot of I_p versus $v^{1/2}$ is linear and intercepting the origin, this process is controlled by diffusion [40]. In the range 20 to 500 $\text{mV}\cdot\text{s}^{-1}$,

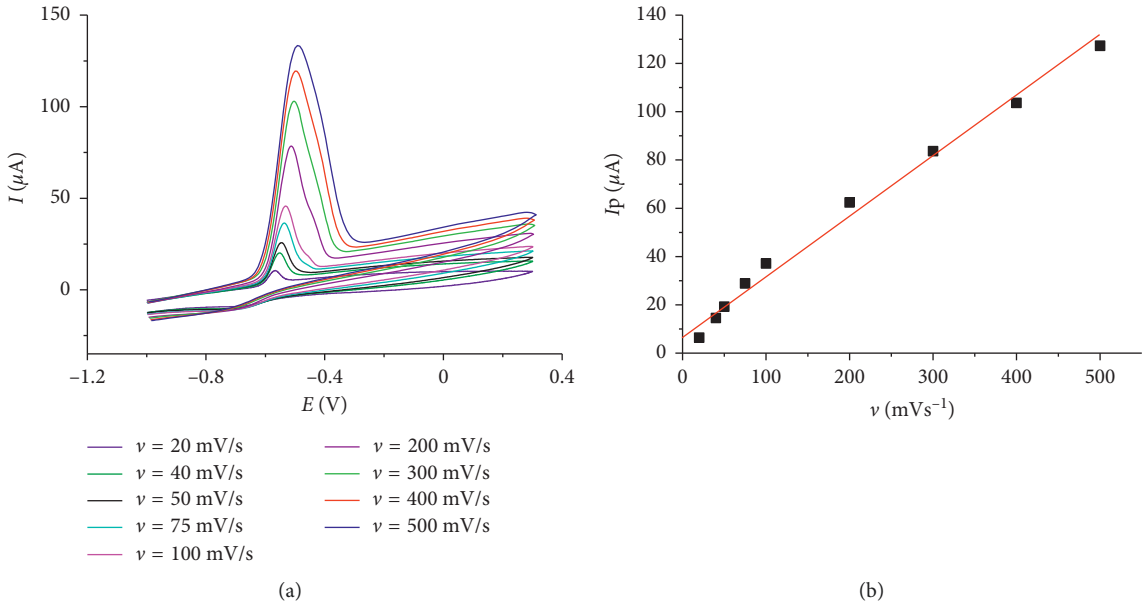

Figure 7: (a) CVs of BiF/Naf/ZiF-8/GCE with an increase in the scan rate from inner to outer: 20–500 mV·s^{-1}; (b) linear regression of I_p versus v.

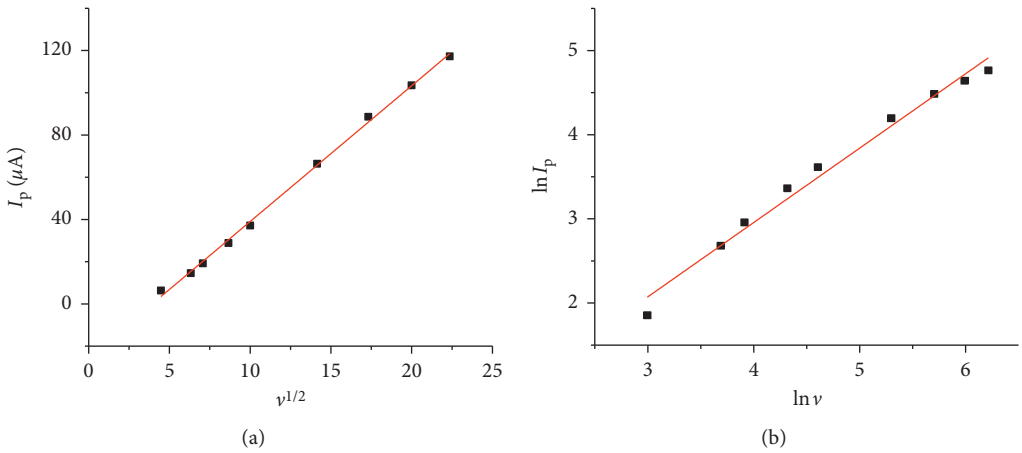

Figure 8: Dependence of anodic peak current (I_p) on potential scan rate$^{1/2}$ ($v^{1/2}$) (a); plot of ln I_p against ln v (b).

I_p of lead electrooxidation varied lineally on $v^{1/2}$ and was expressed by the following:

$$I_p = (0.048 \pm 0.001)v^{1/2} + (-0.641 \pm 0.004). \quad (2)$$

Even the plot of I_p on $v^{1/2}$ as shown in Figure 8(a) was linear ($R = 0.999$; $p \leq 0.001$), the intercept does not cross the origin because 95% confidence interval ((−0.645) to (−0.637)) for intercept does not contain zero. It means that the electrode process of lead electrooxidation was not controlled by the diffusion process.

On the other hand, the slope of linear regression line for ln I_p and ln v can provide information about the diffusion- or adsorption-controlled process. A slope close to 1 is expected for the adsorption-controlled electrode process while close to 0.5 for the diffusion-controlled process [40], a linear relation with high relative coefficient ($R = 0.985$, $p \leq 0.001$) was obtained as shown in Figure 8(b) and is expressed as follows:

$$\ln I_p = (0.883 \pm 0.099)\ln v + (-0.577 \pm 0.477). \quad (3)$$

Then, its slope of 0.883 is close to 1. Then, it was concluded that the oxidation of Pb(II) on the modified electrode was an adsorption-controlled process.

Effective surface area of the modified electrode could be obtained based on the relation between current-potential characteristics. According to the Bard and Faulkner equation [41], the relation between current and potential of the oxidation irreversible process is described by the following equation:

$$I_p = 0.227 \cdot \text{F.A.C.} \exp\left(\frac{\alpha F}{\text{RT}} \cdot E_p\right), \quad (4)$$

where I_p is the current peak (A), E_p is the potential peak (V), A is the effective surface area (cm^2), C is the bulk concentration of Pb(II) (ppb), α is the electron transfer coefficient, F is equal to 96,493 (C mol^{-1}), R is the gas constant

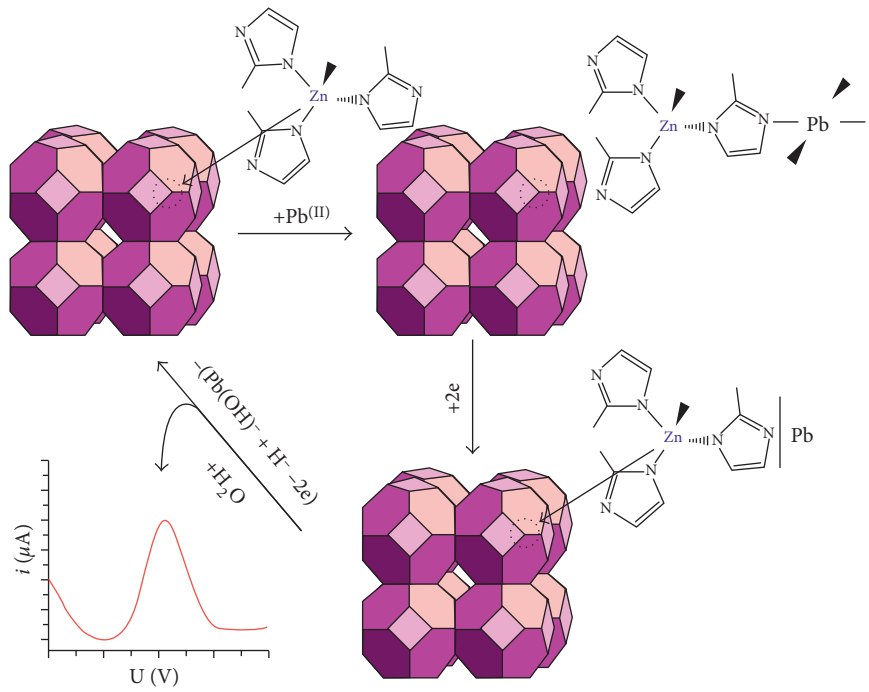

Figure 9: Proposed mechanisms of electrochemistry process for Pb(II) determination at the ZiF-8-based modified electrode by DP-ASV.

to 8.314 ($J{\cdot}K^{-1}$ mol^{-1}), and T is the temperature in Kelvin (298 K).

Natural logarithm (4) obtained the dependence below:

$$\ln I_p = \ln(0.227 \cdot \text{F.A.C}) + \frac{\alpha F}{RT} \cdot E_p. \quad (5)$$

Plot of the linear relation between $\ln I_p$ and E_p provides a linear regression equation as follows:

$$\ln I_p = -25.27 + 6.431 \cdot E_p, \quad R = 0.999. \quad (6)$$

Effective surface area of the modified electrode which was obtained for the intercept of linear regression line was 48.34 cm^2. The geometry surface area of the electrode is 0.065 cm^2 (diameter of the electrode = 2.8 mm). Then, effective surface area was 780 times the geometry surface area of the electrode. The modified electrode with increased surface is due to the presence of ZIF-8. The larger effective surface area results in more active sites and leads to a higher signal-to-nose ratio [42].

The electron transfer rate constant (k_s) was calculated based on the Laviron equation [43]:

$$E_p = E_o + \frac{RT}{\alpha nF} \ln \frac{\alpha nF}{RTK_s} + \frac{RT}{\alpha nF} \ln \nu, \quad (7)$$

where n is the electron transfer number.

The plot of anodic peak potential (E_p) against $\ln \nu$ gives the linear regression equation as follows:

$$E_p\,(\text{V}) = -0.641 + 0.024 \ln \nu. \quad (8)$$

The linear regression with high relative coefficient ($R = 0.996$) was obtained. The value of $n\alpha$ is 1.07 which was obtained from the slope of the regression equation.

The relation between E_{ap} and ν could be analyzed by the model:

$$y = y_0 + A_1 \cdot e^{-x/t_1} + A_2 \cdot e^{-x/t_2}. \quad (9)$$

The nonlinear regression through this model provided the following equation:

$$E_{ap} = -0.478 + (-0.050) \cdot e^{-\nu/29.8} + (-0.071) \cdot e^{-\nu/324.6}; \quad R = 0.998. \quad (10)$$

The high relative coefficient confirmed that this model fitted well experimental data. The standard potential ($E^0_{Pb^{2+}/Pb} = -0.599$ V) with reference electrode Ag/AgCl/KCl 1 M can be the deduced intercept of E_p versus ν on the ordinate by extrapolating the line to $\nu = 0$. The value $K_s = 0.27\ s^{-1}$ could be obtained from the value of intercept and $n\alpha = 1.07$. Since the value of α is assumed to be equal to 0.5, which is commonly employed for a totally irreversible system [44], the value of n was calculated to be 2.14. Therefore, the average number of electrons transferred, n, was 2 which confirmed again that two electrons and one proton were involved in the oxidation of Pb(II) on the ZIF-8-based modified electrode.

The imime groups of imidazole in ZIF-8 bind Pb(II) to surface complexes because of its high affinity to Pb(II) ions [45]. The Pb(II) were accumulated in the electrode due to the reduction reaction and then dissolved in solution through the oxidation reaction. The electrochemical reactions could occur as follows:

Complex step: $\text{ZIF} - 8 + (\text{Pb}(\text{II})) \leftrightarrow \text{ZIF} - 8\,(Pb\,(\text{II}))$

Accumulation step:
$\text{ZIF} - 8\,(\text{Pb}\,(\text{II})) + 2e \leftrightarrow \text{ZIF} - 8\,(\text{Pb}^0)$

Stripping step:
$\text{ZIF} - 8\,(Pb^0) + \text{H}_2\text{O} \leftrightarrow \text{ZIF} - 8 + \text{Pb}\,(\text{OH})^+ + \text{H}^+ + 2e$

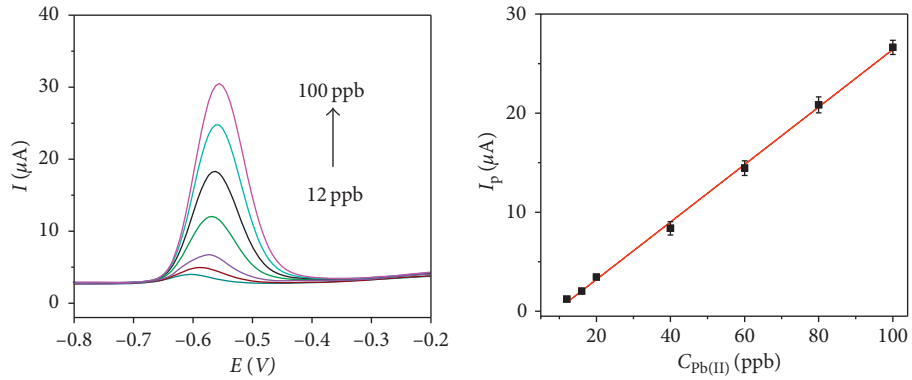

Figure 10: (a) The DP-ASV curves of Pb(II) with increasing Pb(II) from 12 to 100 ppb; (b) the linear regression of I_p versus $C_{Pb(II)}$.

Table 1: A comparison of Pb(II) detection using modified electrodes.

Modified electrodes	Method	Linear range (ppb)	LOD (ppb)	References
MIL-101(Cr)/GCE	SW-ASV	0–207	9.11	[47]
GA/CTS/CNTPE	SW-AdSV	20–414	11.79	[48]
NPC-nafion/Bi/GCE	DP-ASV	7–70	0.80	[49]
BiNPs/GCE	DP-ASV, ABS	5.0–60.0	0.80	[50]
Diatomite-MPTMS/GCE	DP-ASV; ABS	20–150	6.90	[51]
AuNPs/GCE DP	ASV, ABS	—	11.20	[52]
BiF/Naf-ZIF-8/GCE	DP-ASV	12–100	4.16	This study

AuNPs: gold nanoparticles, GA: glutaraldehyde, CPE: carbon paste electrode, BiNPs: nanoparticles bismuth, MPTMS: 3-mercaptopropyl trimethoxysilane, GNFs: graphite nanofibers, CNTPE: carbon nanotube paste electrode, CTS: chitosan, SW-AdSV: square-wave adsorptive stripping voltammetry, DP-ASV: differential pulse-anodic stripping voltammetry, GCE: glass carbon electrode, NPC: nanoporous carbon material.

The electrochemistry process at the ZIF-8-based modified electrode was illustrated in Figure 9.

3.2.3. Repeatability, Reproducibility, Accuracy, Linear Range, and Limit of Detection (LOD). The repeatability of Naf/BiF/ZIF-8/GCE for DP-ASV was checked with the solution of 20 and 100 ppb Pb (II). The detection of 20 and 100 ppb Pb (II) in each signal was estimated by successive measurements for seven times. The obtained RSD for 20 and 100 ppb were 7.08 and 3.92%, respectively, that were lower than the 1/2 $RSD_{Horwitz\ predicted}$ [46]. Such reasonable RSD of successive measurements demonstrated that the Naf/BiF/ZIF-8/GCE could be repeatedly used for the detection of Pb(II) in either low concentration range or high concentration range. The reproducibility was also estimated with five Naf/BiF/ZIF-8/GCEs in detection of 20 ppb Pb(II) under the optimized conditions. The results exhibited a good reproducibility with the RSD of the current responses as 7.0%. The expectable RSD for five independent electrodes confirmed the good reproducibility of the obtained Naf/BiF/ZIF-8/GCE.

The accuracy of the method was estimated through the recovery of a spike of Pb(II). The solution with known concentration was prepared from stock solution. The 100 μL of 10 ppm Pb(II), 30 mL of 100 ppm Bi(III), and 1 mL of 0.5 M B-R buffet (pH = 3.2) were mixed together and diluted to 100 mL. This solution was split into two portions. The concentration of one portion evaluated by DP-ASV under optimal condition was 9.59 ppb. The other was spiked for increasing the concentration by 10 ppb. The concentration of Pb(II) in spiked solution determined by DP-ASV under optimum conditions was 20.69 ppb. Recovery (% Rev) was 110.1%. This result suggested that the determination of Pb (II) employing the DP-ASV with BiF/Naf-ZiF-8/GCE possessed acceptable error [35].

Under the optimal conditions, the linear range of lead detection with a ZIF-8- modified electrode was conducted. The response current peak (I_p) was linear in the concentration range 12 ppb to 100 ppb ($R = 0.999$) as shown in Figure 10(a). Linear regression equation of the calibration curves was $I_p = (-2.601 \pm 0.697) + (0.290 \pm 0.012)\ C_{Pb(II)}$ (Figure 10(b)). Sensitivity obtained from the slope of the calibration curve was 0.290 μA/ppb. The limit of detection (LOD) was calculated based on the concentration from 12 ppb to 100 ppb. As shown in Figure 10(b) the LOD was calculated from 3 S_y/b, where S_y is the standard deviation of y-residuals and b is the slope of linearity. The LOD was found to be 4.16 ppb. The limit of quantitation (LOQ) calculated from 10 S_y/b was 13.9 ppb.

The obtained detection limits and the linear ranges in this work were compared with the results reported previously, in which the electrode was modified with gold nanoparticle-graphene-cysteine composite, chitosan, MIL-100, polyaniline, bismuth nanoparticles, and mercapto-diatomite composite [47–52]. A comparison was listed in Table 1. It could be noticed that the detection limit of Pb(II) from the Nafion/BiF/ZIF-8/GCE electrode was lower or

comparable with those results based on modified electrodes in previous papers. The ZIF-8-modified electrode exhibited better than some of the electrodes based on kaolinite, MPTMS-diatomite, or gold nanoparticles but failed to some others. Overall, the ZIF-8 was proved to be an effective electrode modifier for the detection of Pb(II) in aqueous solution.

4. Conclusions

A novel electrode modifier named zeolite imidazole framework-ZIF-8 has been prepared by a hydrothermal process. ZIF-8 was stable in ambient atmosphere and water. It is stable in pH ranging from 3 to 12 and exhibits the remarkable chemical resistance to some boiling organic solvents. The obtained ZIF-8 was applicable to the fabrication of an BiF-Naf/ZIF-8/GCE composite electrode, which gave a good performance in the determination of Pb(II) using the DP-ASV technique due to a combination of the advantages of ZIF-8 with high surface area, hierarchical porous structure, and thermal and chemical stabilities. The peak current of Pb(II) was linearly proportional to its concentration over the range of 12 to 100 ppb. The limit of detection and the limit of quantitation were as low as 4.12 ppb and 12.50 ppb, respectively. These results showed that ZIF-8 is a potential electrode modifier for lead determination in aqueous solution.

Conflicts of Interest

The authors declare that they have no conflicts of interest.

Acknowledgments

This work was supported by the project B2016-DHH-20 sponsored by the Ministry of Education and Training, Vietnam.

References

[1] L. C. Jesse, R. Andrew, R. Millward, K. S. Park, and O. M. Yaghi, "Hydrogen sorption in functionalized metal–organic frameworks," *Journal of the American Chemical Society*, vol. 126, no. 18, pp. 5666-5667, 2004.

[2] I. Luz, F. X. Llabrés i Xamena, and A. Corma, "Bridging homogeneous and heterogeneous catalysis with MOFs: "click" reactions with Cu-MOF catalysts," *Journal of Catalysis*, vol. 276, no. 1, pp. 134–140, 2010.

[3] M. Opanasenko, A. Dhakshinamoorthy, M. Shamzhy et al., "Comparison of the catalytic activity of MOFs and zeolites in Knoevenagel condensation," *Catalysis Science and Technology*, vol. 3, no. 2, pp. 500–507, 2013.

[4] R. Banerjee, A. Phan, B. Wang, C. Knobler, H. Furukawa, and M. O'Keeffe, "High-throughput synthesis of zeolitic imidazolate frameworks and application to CO_2 capture," *Science*, vol. 319, no. 5865, pp. 939–943, 2008.

[5] S. R. Venna and M. A. Carreon, "Highly permeable zeolite imidazolate framework-8 membranes for CO_2/CH_4 separation," *Journal of the American Chemical Society*, vol. 132, no. 1, pp. 76–78, 2010.

[6] A. K. Kida, M. Okita, K. Fujita, S. Tanaka, and Y. Miyake, "Formation of high crystalline ZIF-8 in an aqueous solution," *CrystEng Comm*, vol. 15, no. 9, pp. 1794–1801, 2013.

[7] D. Yamamoto, T. Maki, S. Watanabe, H. Tanaka, M. T. Miyahara, and K. Mae, "Synthesis and adsorption properties of ZIF-8 nanoparticles using a micromixer," *Chemical Engineering Journal*, vol. 227, pp. 145–150, 2013.

[8] H. Bux, A. Feldhoff, J. Cravillon, M. Wiebcke, Y.-S. Li, and J. Caro, "Oriented zeolitic imidazolate framework-8 membrane with sharp H_2/C_3H_8 molecular sieve separation," *Chemistry of Materials*, vol. 23, no. 8, pp. 2262–2269, 2011.

[9] H. Wu, W. Zhou, and T. Yildirim, "Hydrogen storage in a prototypical zeolitic imidazolate framework-8," *Journal of the American Chemical Society*, vol. 129, no. 17, pp. 5314-5315, 2007.

[10] B. Assfour, S. Leoni, G. Seifer, and J. Phys, "Hydrogen adsorption sites in zeolite imidazolate frameworks ZIF-8 and ZIF-11," *Journal of Physical Chemistry C*, vol. 114, no. 17, pp. 13381–13384, 2010.

[11] M. T. Luebbers, T. Wu, L. Shen, and R. I. Masel, "Effects of molecular sieving and electrostatic enhancement in the adsorption of organic compounds on the zeolitic imidazolate framework ZIF-8," *Langmuir*, vol. 26, no. 19, pp. 15625–15633, 2010.

[12] U. P. N. Tran, K. K. A. Le, and N. T. S. Phan, "Expanding applications of metal–organic frameworks: zeolite imidazolate framework ZIF-8 as an efficient heterogeneous catalyst for the knoevenagel reaction," *ACS Catalysis*, vol. 1, no. 2, pp. 120–127, 2011.

[13] C. M. Miralda, E. E. Macias, M. Zhu, P. Ratnasamy, and M. A. Carreon, "Zeolitic imidazole framework-8 catalysts in the conversion of CO_2 to chloropropene carbonate," *ACS Catalysis*, vol. 2, no. 1, pp. 180–183, 2012.

[14] M. M. Abdel-Galeil, M. M. Ghoneim, H. S. El-Desoky, T. Hattori, and A. Matsuda, "Anodic stripping voltammetry determination of lead ions using highly sensitive modified electrodes based on multi-walled carbon nanotube," *Journal of Chemistry and Biochemistry*, vol. 2, no. 2, pp. 25–43, 2014.

[15] S. Morante-Zarcero, A. Sánchez, M. Fajardo, I. Hierro, and I. Sierra, "Voltammetric analysis of Pb(II) in natural waters using a carbon paste electrode modified with 5-mercapto-1-methyltetrazol grafted on hexagonal mesoporous silica," *Microchimica Acta*, vol. 169, pp. 57–64, 2010.

[16] F. Barbosa, F. J. Krug, and É. C. Lima, "On-line coupling of electrochemical preconcentration in tungsten coil electrothermal atomic absorption spectrometry for determination of lead in natural waters," *Spectrochimica Acta Part B: Atomic Spectroscopy*, vol. 54, no. 8, pp. 1155–1166, 1999.

[17] J. Vogl and K. G. Heumann, "Determination of heavy metal complexes with humic substances by HPLC/ICP-MS coupling using on-line isotope dilution technique," *Fresenius' Journal of Analytical Chemistry*, vol. 359, no. 4-5, pp. 438–441, 1997.

[18] D. W□grzynek and B. Hołyńska, "Simultaneous analysis of trace concentrations of lead and arsenic by energy-dispersive X-ray fluorescence spectrometry," *Applied Radiation and Isotopes*, vol. 44, no. 8, pp. 1101–1104, 1993.

[19] A. Phan, C. J. Doonan, F. J. Uribe-Romo, C. B. Knobler, M. O'Keeffe, and O. M. Yaghi, "Synthesis, structure, and carbon dioxide capture properties of zeolitic imidazolate frameworks," *Accounts of Chemical Research*, vol. 43, no. 1, pp. 58–67, 2010.

[20] L. Xiao, H. Xu, S. Zhou et al., "Simultaneous detection of Cd(II) and Pb(II) by differential pulse anodic stripping voltammetry at a nitrogen-doped microporous carbon/Nafion/bismuth-film electrode," *Electrochimica Acta*, vol. 143, pp. 143–151, 2014.

[21] A. Walcarius, "Mesoporous materials-based electrochemical sensors," *Electroanalysis*, vol. 27, no. 6, pp. 1303–1340, 2015.
[22] A. Magheara, M. Etienne, M. Tertis, R. S. Andulescu, and A. Walcarius, "Clay-mesoporous silica composite films generated by electro-assisted self-assembly," *Electrochimica Acta*, vol. 112, pp. 333–341, 2013.
[23] V. P. Pattar and S. T. Nandibewoor, "Electroanalytical method for the determination of 5-fluorouracil using a reduced graphene oxide/chitosan modified sensor," *RSC Advances*, vol. 5, no. 43, pp. 34292–34301, 2015.
[24] J. I. Gowda and S. T. Nandibewoor, "Simultaneous electrochemical determination of 4-aminophenazone and caffeine at electrochemically pre-treated graphite pencil electrode," *Analytical Methods*, vol. 6, pp. 5147–5154, 2014.
[25] A. M. Bagoji and S. T. Nandibewoor, "Electrocatalytic redox behavior of graphene films towards acebutolol hydrochloride determination in real samples," *New Journal of Chemistry*, vol. 40, no. 4, pp. 3763–3772, 2016.
[26] V. P. Pattar and S. T. Nandibewoor, "Staircase voltammetric determination of 2-thiouracil in pharmaceuticals and human biological fluids at polyaniline and polypyrrole film modified sensors," *Sensors and Actuators A: Physical*, vol. 250, pp. 40–47, 2016.
[27] J. Mao, L. Yang, P. Yu, X. Wei, and L. Mao, "Electrocatalytic four-electron reduction of oxygen with copper (II)-based metal-organic frameworks," *Electrochemistry Communications*, vol. 19, pp. 29–31, 2012.
[28] H. Hosseini, H. Ahmar, A. Dehghani, A. Bagheri, A. R. Fakhari, and M. M. Amini, "Au-SH-SiO_2 nanoparticles supported on metal-organic framework (Au-SH-SiO_2@Cu-MOF) as a sensor for electrocatalytic oxidation and determination of hydrazine," *Electrochimica Acta*, vol. 88, pp. 301–309, 2013.
[29] Y. Wang, H. Ge, Y. Wu, G. Y. H. Chen, and X. Hu, "Construction of an electrochemical sensor based on amino-functionalized metal-organic frameworks for differential pulse anodic stripping voltammetric determination of lead," *Talanta*, vol. 129, pp. 100–105, 2014.
[30] A. Samadi-Maybodi, S. Ghasemi, and H. Ghaffari-Rad, "A novel sensor based on Ag-loaded zeolitic imidazolate framework-8 nanocrystals for efficient electrocatalytic oxidation and trace level detection of hydrazine," *Sensors and Actuators B: Chemical*, vol. 220, pp. 627–633, 2015.
[31] N. H. Phong, M. T. Thanh, D. C. Tien, M. X. Tinh, N. P. Hung, and D. Q. Khieu, "Assess the status of exposure workers to benzene, toluene by analysis the metabolites products in the urine," *VNU Journal of Science: Natural Sciences and Technology*, vol. 32, no. 1, pp. 198–206, 2016.
[32] H.-Y. Cho, J. Kim, S.-N. Kim, and W.-S. Ahn, "High yield 1-L scale synthesis of ZIF-8 via a sonochemical route," *Microporous and Mesoporous Materials*, vol. 169, pp. 180–184, 2013.
[33] M. Zhua, D. Srinivas, S. Bhogeswararao, P. Ratnasamy, and M. A. Carreon, "Catalytic activity of ZIF-8 in the synthesis of styrene carbonate from CO_2 and styrene oxide," *Catalysis Communications*, vol. 32, pp. 36–40, 2013.
[34] M. Zhu, S. R. Venna, J. B. Jasinski, and M. A. Carreon, "Room-temperature synthesis of ZIF-8: the coexistence of ZnO nanoneedles," *Chemistry of Materials*, vol. 23, no. 16, pp. 3590–3592, 2011.
[35] D. Harvey, *Modern Analytical Chemistry*, McGraw-Hill Higher Education, New York, NY, USA, 2000.
[36] S. Eslava, L. Zhang, S. Esconjauregui et al., "Metal-organic framework ZIF-8 films as low-κ dielectrics in microelectronics," *Chemistry of Materials*, vol. 25, no. 1, pp. 27–33, 2013.
[37] Y. Du, R. Z. Chen, J. F. Yao, and H. T. Wang, "Facile fabrication of porous ZnO by thermal treatment of zeolitic imidazolate framework-8 and its photocatalytic activity," *Journal of Alloys and Compounds*, vol. 551, pp. 125–130, 2013.
[38] F. Torma, M. Kádár, K. Tóth, and E Tatár, "Nafion®/2,2′-bipyridyl-modified bismuth film electrode for anodic stripping voltammetry," *Analytica Chimica Acta*, vol. 619, no. 2, pp. 173–182, 2008.
[39] L. Fotouhi, M. Fatollahzadeh, and M. M. Heravi, "RETRACTED: "Mahendra Yadav, Sushil Kumar, Indra Bahadur, Deresh Ramjugernath, Electrochemical and quantum chemical studies on synthesized phenylazopyrimidone dyes as corrosion inhibitors for mild steel in a 15% HCl Solution [Int. J. Electrochem. Sci., 9 (2014) 3928 - 3950]"," *International Journal of Electrochemical Science*, vol. 7, pp. 3919–3928, 2012.
[40] J. Soleymani, M. Hasanzadeh, N. Shadjou et al., "A new kinetic–mechanistic approach to elucidate electrooxidation of doxorubicin hydrochloride in unprocessed human fluids using magnetic graphene based nanocomposite modified glassy carbon electrode," *Materials Science and Engineering C*, vol. 61, pp. 638–650, 2016.
[41] A. J. Bard and L. R. Faulkner, *Fundamentals and Applications: Electrochemical Methods*, John Wiley & Sons Inc., Hoboken, NJ, USA, 2nd edition, 2001.
[42] G. Yang, X. Qu, M. Shen, C. Wang, Q. Qu, and X. Hu, "Electrochemical behavior of lead(II) at poly(phenol red) modified glassy carbon electrode, and its trace determination by differential pulse anodic stripping voltammetry," *Microchimica Acta*, vol. 160, no. 1-2, pp. 275–281, 2008.
[43] E. Laviron, "General expression of the linear potential sweep voltammogram in the case of diffusionless electrochemical systems," *Journal of Electroanalytical Chemistry and Interfacial Electrochemistry*, vol. 101, pp. 19–28, 1979.
[44] C. Li, "Electrochemical determination of dipyridamole at a carbon paste electrode using cetyltrimethyl ammonium bromide as enhancing element," *Colloids and Surfaces B: Biointerfaces*, vol. 55, pp. 77–83, 2007.
[45] D. Mallick, U. Panda, S. Jana, C. Sen, T. K. Mondal, and C. Sinha, "Lead(II) complexes of 1-alkyl-2-(arylazo)imidazole: synthesis, structure, photochromism and metallomesogenic properties," *Polyhedron*, vol. 117, pp. 318–326, 2016.
[46] W. Horwitz and R. Albert, "Quality issues the concept of uncertainty as applied to chemical measurements," *Analyst*, vol. 122, no. 6, pp. 615–617, 1997.
[47] D. Wang, Y. Ke, D. Guo, H. Guo, and J. Chen, "Facile fabrication of cauliflower-like MIL-100(Cr) and its simultaneous determination of Cd2+, Pb2+, Cu2+ and Hg2+ from aqueous solution," *Sensors and Actuators B: Chemical*, vol. 216, pp. 504–510, 2015.
[48] F. C. Vicentini, T. A. Silva, A. Pellatieri, and B. C. Janegitz, "Pb (II) determination in natural water using a carbon nanotubes paste electrode modified with crosslinked chitosan," *Microchemical Journal*, vol. 116, pp. 191–196, 2014.
[49] L. Xiao, S. Zhou, G. Hu, H. Xu, Y. Wang, and Q. Yuan, "One-step synthesis of isoreticular metal–organic framework-8 derived hierarchical porous carbon and its application in differential pulse anodic stripping voltammetric determination of Pb(ii)," *RSC Advances*, vol. 5, no. 94, pp. 77159–77167, 2015.
[50] D. Yang, L. Wang, Z. Chen, M. Megharaj, and R. Naidu, "Anodic stripping voltammetric determination of traces of Pb (II) and Cd(II) using a glassy carbon electrode modified with bismuth nanoparticles," *Microchimica Acta*, vol. 181, no. 11-12, pp. 1199–1206, 2014.
[51] D. Q. Khieu, B. H. Son, V. T. T. Chau, P. D. Du, N. H. Phong, and N. T. D. Chau, "3-Mercaptopropyltrimethoxysilane Modified Diatomite: Preparation and Application for Voltammetric

Determination of Lead (II) and Cadmium (II)," *Journal of Chemistry*, vol. 2017, article 9560293, 10 pages, 2017.

[52] X. Xu, G. Duan, Y. Li et al., "Fabrication of gold nanoparticles by laser ablation in liquid and their application for simultaneous electrochemical detection of Cd2+, Pb2+, Cu2+, Hg2+," *ACS Applied Materials and Interfaces*, vol. 6, no. 1, pp. 65–71, 2014.